

## A Fatigue Damage Model for FRP Composite Laminate Systems Based on Stiffness Reduction

Ying Zhao<sup>1</sup>, Mohammad Noori<sup>1,2</sup>, Wael A. Altabey<sup>1,3,\*</sup>, Ramin Ghiasi<sup>4</sup>  
and Zhishen Wu<sup>1</sup>

**Abstract:** This paper introduces a stiffness reduction based model developed by the authors to characterize accumulative fatigue damage in unidirectional plies and (0/θ/0) composite laminates in fiber reinforced polymer (FRP) composite laminates. The proposed damage detection model is developed based on a damage evolution mechanism, including crack initiation and crack damage progress in matrix, matrix-fiber interface and fibers. Research result demonstrates that the corresponding stiffness of unidirectional composite laminates is reduced as the number of loading cycles progresses. First, three common models in literatures are presented and compared. Tensile viscosity, Young's modulus and ultimate tensile stress of composites are incorporated as key factors in this model and are modified in accordance with temperature. Four types of FRP composite property parameters, including Carbon Fiber Reinforced Polymer (CFRP), Aramid Fiber Reinforced Polymer (AFRP), Glass Fiber Reinforced Polymer (GFRP), and Basalt Fiber Reinforced Polymer (BFRP), are considered in this research, and a comparative parameter study of FRP unidirectional composite laminates with different off-angle plies using control variate method are discussed. It is concluded that the relationship between the drop in stiffness and the number of cycles also shows three different regions, following the mechanism of damage of FRP composites and the matrix is the dominant factor determined by temperature, while fiber strength is the dominant factor that determine the reliability of composite.

**Keywords:** FRP laminates, fatigue damage model, stiffness reduction, thermal effect.

### 1 Introduction

In recent years, fiber reinforced polymer composites have received rapidly increasing attention and application in structural systems. This has been mainly due to their high

---

<sup>1</sup> International Institute for Urban Systems Engineering (IIUSE), Southeast University, Nanjing, China.

<sup>2</sup> Mechanical Engineering Department, California Polytechnic State University, San Luis Obispo, CA 93405, USA.

<sup>3</sup> Mechanical Engineering Department, Faculty of Engineering, Alexandria University, Alexandria, 21544, Egypt.

<sup>4</sup> Department of Civil Engineering, Faculty of Engineering, University of Sistan and Baluchestan, Zahedan, Iran.

\* Corresponding Author: Wael A. Altabey. Email: wael.atabey@gmail.com.

strength / weight ratio, and corrosion resistance that are superior over other traditional materials such as concrete and steel. Owing to good research and applied value, they have been successfully used in a wide fields of civil, aerospace and automotive engineering. A large number of analytical and experimental work regarding fatigue and creep damage mechanism and mathematical model, durability, reliability and long term performance assessment under normal and extreme conditions has been carried out.

Detailed studies on FRP composite damage types, damage evolution mechanism and related models can be summarized as follows. The main failure types for pipeline systems, including attachment joint, corrosion-induced, impact, temperature-induced, bend, tensile, and stress failure, as well as improper installation and other failure modes have been extensively reviewed [Liu, Shao, Han et al. (2009); Altabey (2017)]. Accordingly, different damage mechanisms have been analyzed and evaluated for unidirectional carbon fiber reinforced epoxy matrix composites under off-axis cyclic loading [Plumtree and Shi (2002)]. Damage growth in composite laminates has also been extensively studied via experimental research in four different modes: micro-damage, delamination, matrix cracking, and fiber failure [Wharmby, Ellyin and Wolodko (2003); Altabey (2017a, 2017b)]. Moreover, progressive damage method has been utilized to predict the static mechanical properties of FRP composite laminates [Sun, Zhang and Fei (2011)]. Stiffness reduction based mechanisms in composite laminates have also been investigated [Praveen and Reddy (1995)] and an algorithm for progressive damage simulation for performance evaluation of GFRP composites under cyclic loads for material constitutive model and model validation has been introduced in the literature [Eliopoulos and Philippidis (2011a, 2011b)]. The influence of other parameters on the stress concentrations, including the interfacial shear strength and matrix-to-fiber tensile stiffness ratio, and the extent of damaged regions at the interface, have also been investigated and reported [Zeng, Wang and Ling (1997)]. Moreover, a criterion for the non-fibre controlled fatigue behavior of unidirectional laminate under multiaxial loading has been proposed [Carraro and Quaresimin (2014)] and a multiaxial fatigue damage model for fibre reinforced polymer (FRP) composite materials has been introduced which combines the fatigue-induced fibre strength and modulus degradation, irrecoverable cyclic strain effects and inter-fibre fatigue [Kennedy, O'Bradaigh and Leen (2013)].

Extensive work has also been reported in the literature pertaining to the damage detection of FRP composites. For instance, an artificial neural network (ANN) based method which takes into account the effect of the residual strength from spectrum loading has been reported which can predict the fatigue life of carbon fibre/epoxy composite laminate sheets involving 12 balanced woven bidirectional layers with the same orientation angle  $[0/90^\circ]$  as they are subjected to variable amplitude block loadings with different negative and positive stress ratios [Altabey and Noori (2017)]. This proposed ANN scheme has been able to predict the fatigue behavior of woven-roving glass fiber reinforced epoxy (GFRE) composites with fiber orientations of  $[0, 90^\circ]_{3s}$  and  $[\pm 45^\circ]_{3s}$  under combined bending moments and internal hydrostatic pressure. The pressure ratios considered have been between the applied pressure and the burst pressure  $P_r=0.25, 0.5$  and  $0.75$  [Abouelwafa, El-Gamal, Mohamed et al. (2014)].

In other studies related to the damage detection and prediction, a finite element pipeline model was developed for the case when the pipeline was under the coupled structural-thermal-electrostatic field. This model was utilized to investigate a case involving the damage identification of carbon fiber-reinforced polymer (CFRP) composite piping systems. Based on this model, a cumulative damage model was introduced to model the fatigue damage to the pipeline. In that study ten cases of damage were considered [Zhao, Noori, Altabey et al. (2018)]. The mechanical properties of polymers and polymer matrix composites can be affected by water absorption, “Altabey et al. [Altabey and Noori (2018)] detected the absorption rate and computing the mass of water absorption (M%) as a function of absorption time (t) in glass-fiber reinforced Epoxy (GFRE) composite pipes”.

Two physical damage cumulative models, strength evolution integral model and cumulative damage formalism model, were used to make a comparison between the classical and empirical Linear Cumulative Damage law, and predict fatigue lifetime of composite laminates [Guedes (2008)]. Some numerical and experimental work regarding reinforced concrete with strengthened FRP has been in progress. Finite element analysis has been utilized to simulate the fatigue damage evolution in composite laminates in order to predict the fatigue life of laminates with different lay-up sequences based on the fatigue characteristics of transverse, longitudinal, and in-plane shear directions [Lian and Yao (2010)]. Another finite element model has also been developed to simulate the onset and the growth of damage due to delamination in laminated FRP composite bonded tubular single lap joints [Das and Pradhan (2013)]. In that study, an analysis of three-dimensional stresses was carried out to investigate the fracture behavior of bonded composite pipe joints under internal pressure and axial loading [DasN and Baishya (2016)]. In another study, in order to investigate the behavior of FRP reinforced concrete structures, the adhesion property was reconstructed through a contact model incorporating an elastic-damaged constitutive law that could related the inter-laminar stresses acting in the sliding direction [Mazzucco, Salomoni and Majorana (2012)]. In addition, a new concept, namely, damage- or crack-band, was introduced in order to predict the failure due to de-bonding of the concrete-epoxy interface when FRP sheets, or plates, were externally bonded to a concrete substrate [Coronado and Lopez (2010); Altabey and Noori (2017)]. A damage modelling approach was also employed [Ruocci, Argoul, Benzarti et al. (2013)] considering the variability of fracture mechanisms in FRP reinforced concrete structures, that is a three-domain system with concrete, glue and FRP reinforcement assumed as damageable materials connected together via two interfaces. A damage identification approach was also proposed by using FE model updating of a GFRP composite beam. This study compared the numerical results of the FRP structure to the experimental results with proper correlation [Adediran, Abdel Wahab, Xu et al. (2018)]. Further studies have included an experimental investigation that assessed the effect of CFRP, GFRP and BFRP materials on the strengthening effectiveness of reinforced concrete slabs [Chen, Wan, Lee et al. (2008)].

An important issue that should be considered in the damage detection study of FRP composites is if it is possible, or feasible, to detect the damage as quickly as possible so that we can monitor, evaluate and repair the structure if necessary. This control strategy is an integral component of a broader framework, or the context, for structural health monitoring. In order to address these two objectives, vibration based SHM methodologies

can be considered. The main objective of vibration analysis based damage detection is to exploit the dynamic response of a structure in order to detect damage [Altabey (2017a, 2017b); Altabey (2018); Altabey (2014)].

As discussed, despite the fact that extensive theoretical and experimental research have been conducted to study on the basic FRP properties, the accumulative fatigue damage model considering thermal effect have not been fully developed yet. More recently, a fatigue-damage model was proposed to assess the stiffness degradation in composite materials, and under a wide range of loading levels [Shiri, Yazdani and Pourgol-Mohammad (2015)]. An experimental work including static and fatigue tests demonstrated that different off-axis directions had different properties for multidirectional glass/polyester laminates [Philippidis and Vassilopoulos (1999)]. A model was also proposed based on physics and the mechanism of fatigue crack development within three damage regions of matrix, fiber-matrix interface, and fiber as the number of cycles progressed [Varvani-Farahani, Haftchenari and Panbechi (2006); Varvani-Farahani, Haftchenari and Panbechi (2007)]. A stiffness reduction damage model was also presented that characterized the fatigue damage of  $0^\circ$  and  $90^\circ$  unidirectional plies and its extension to  $(0^\circ, 90^\circ)$  FRP composite systems. Simultaneously, this approach took into account the effects of the magnitude of cyclic stress, off-axis angle, mean stress and matrix-fiber bonding strength with respect to the cycles of applied stress [Varvani-Farahani and Shirazi (2007)]. Later on a stiffness reduction based model was considered and studied for describing the fatigue damage in unidirectional  $0^\circ$  and  $\theta^\circ$  plies and  $(0^\circ, \theta^\circ)$  laminates of fiber reinforced composites [Shirazi, and Varvani-Farahani (2010)] as well as the temperature effect on cumulative fatigue damage of laminated fiber-reinforced polymer composites. Experimental studies showed a good agreement with the theoretical model [Mivehchi and Varvani-Farahani (2010)]. As a follow up to the aforementioned research, this paper makes a detailed comparative study on the accumulative fatigue-damage model for different types of FRP laminates by considering the effect of temperature.

## **2 Fatigue damage mechanism for FRP composite laminates**

The peculiarity of damage mechanism of FRP composites is characterized by the fact that three constituents (matrix, fiber-matrix interface, and fiber) do not fail simultaneously due to their differing ultimate characteristics [Varvani-Farahani, Haftchenari and Panbechi (2006); Varvani-Farahani, Haftchenari and Panbechi (2007)]. The initiation, development and evolution of progressive damage is generally regarded as a multi-phase phenomenon. Micro damage initiates at the first stage, cyclic tension-compression excursions may probably produce matrix cracks, which is one of the dominant factors that determines the residual strength and fatigue life of a laminate. During fabrication process, local micro-defects are formed in maldistributed voids, misaligned fibers and resin-rich regions. Once initiated, matrix cracks develop and grow in various modes within the matrix over the whole life cycles. Crack damage accumulation continues and extend until it encounters a fiber, concentrating on matrix-fiber interface. At this stage, debonding between matrix and fibers emerges, giving rise to increased reduction in stiffness and strength of a laminate ply. Damage development in the later stage is

characterized by increasing progression rate of various modes of damage that result in significant fiber failure. The progressive damage development during the whole fatigue life is depicted in Fig. 1. In region I, micro cracks within the matrix initiate and concentrate together, constituting the first 20% of fatigue life. In Region II, matrix cracks continue to commence and develop, and reach and approach the neighborhood around fibers. Cracks grow and accumulate along the interface of fiber-matrix with number of cycles increasing, characterized of a lower slope of damage progress during a relatively longer life span. In region III, fiber breakage occurs within a short time duration after the accumulation of damage during regions I and II, which may probability result in component's failure [Plumtree and Shi (2002)].

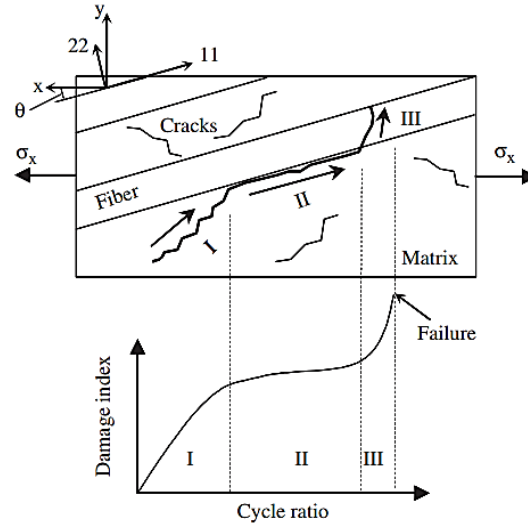


**Figure 1:** Crack progression mechanism in unidirectional composites

### 3 Comparison of residual stiffness fatigue damage models

It is important to mathematically design a model to measure the cumulative damage of composites due to fatigue with respect to Young's module's or stiffness reduction. The quantification of the damage caused by fatigue can be shown as in Tab. 1:

**Table 1:** The Mathematical models of the cumulative fatigue damage of composite materials

No	Mathematical model
1	$D = 1 - \frac{E_N}{E_0} = 1 - K \left( \frac{\sigma_a}{E_0} \right)^c \left( \frac{N}{N_f} \right)$
2	$D = \left\{ \frac{E_m V_m}{E_c} (1 - f^*) \frac{\ln(N+1)}{\ln(N_f)} \right\} + \left\{ \frac{E_m V_m}{E_c} f^* \left( \frac{N}{N_f} \right) \right\} + \left\{ \frac{E_f V_f}{E_c} \left( 1 - \frac{\sigma_{appl}}{\sigma_{ult}} \right) \frac{\ln\left(1 - \frac{N}{N_f}\right)}{\ln\left(\frac{1}{N_f}\right)} \right\}$
3	$D = \left\{ \left( 1 - \frac{E_f V_f \cos \theta}{E_c} \right) (1 - f^*) \frac{\ln(N+1)}{\ln(nN_f)} \right\} + \left\{ \left( 1 - \frac{E_f V_f \cos \theta}{E_c} \right) f^* \left( \frac{N}{nN_f} \right) \right\}$

$$+ \left\{ \frac{E_f V_f \cos \theta}{E_c} \left( \mathbf{1} - \frac{\sigma_{max}(1-R)}{2\sigma_{ult}} \right) \frac{\ln\left(\mathbf{1} - \frac{N}{nN_f}\right)}{\ln\left(\frac{1}{nN_f}\right)} \right\}$$

Remark: <sup>1</sup>Philippidis, <sup>2</sup>Ramkrishnan-Jayaraman, <sup>3</sup>Varvani-Farahani-Shirazi.

### Fatigue Damage Model with Temperature Effect

The aforementioned fatigue damage models include important terms such as important mechanical property parameters of materials however they do not take temperature into consideration. Thus, the model is developed as a function of mainly two factors including both material, structural and coupled field parameters (Young's modulus  $E$ , volume fraction  $V$ , fiber orientation  $\theta$ , interface strength parameter between fiber and matrix  $f^*$ , maximum applied stress  $\sigma_{max}$ , ultimate tensile stress  $\sigma_{ult}$ , load and stress ratio  $R$ , number of loading cycles  $N$  and temperature effect  $T$ )

$$D = D(E_c, E_f, V_f, \theta, f^*, \sigma_{max}, \sigma_{ult}, N, N_f, R, T) \quad (1)$$

Including The parameters  $E_c$ ,  $\sigma_{ult}$  and  $N_f$  were found temperature dependent. As a conclusion, we have:

$$D = \left\{ \left( \mathbf{1} - \frac{E_f V_f \cos \theta}{E_c(T)} \right) (1 - f^*) \frac{\ln(N + 1)}{\ln(nN_f(T))} \right\} + \left\{ \left( \mathbf{1} - \frac{E_f V_f \cos \theta}{E_c(T)} \right) f^* \left( \frac{N}{nN_f(T)} \right) \right\} \\ + \left\{ \frac{E_f V_f \cos \theta}{E_c(T)} \left( \mathbf{1} - \frac{\sigma_{max}(1-R)}{2\sigma_{ult}(T)} \right) \frac{\ln\left(\mathbf{1} - \frac{N}{nN_f(T)}\right)}{\ln\left(\frac{1}{nN_f(T)}\right)} \right\} \quad (2)$$

A shift factor is introduced to describe the temperature effect on mechanical properties of polymers. Here are two equations incorporating thermal effect as shown in Tab. 2:

**Table 2:** Equations of A shift factor to describe temperature effect on mechanical properties of polymers

No	Equation	Application
1	$\log a(T) = \frac{-C_1(T-T_0)}{C_2+T+T_0}$ , $T_g < T < T_g + 100K$ , $C_1$ and $C_2$ are universal constants	viscoelastic and rubbery polymer
2	$\log a(T) = \frac{\Delta H}{2.303G_c} \left( \frac{1}{T} - \frac{1}{T_0} \right)$ , $G_c = 8.314 \left( \frac{J}{K} \text{mol} \right)$ , $T > T_g + 100K$ , $T_0$ is assumed as room temperature	rubber polymer e.g. liquid polymer

Remark: <sup>1</sup> Williams-Landel-Ferry (WLF), <sup>2</sup>Arrhenius.

However, both WLF and Arrhenius equations have disadvantages in that they are usually applied to bulk polymers in temperature above the glass transition temperature, and the experimental measurements are required and necessary for obtaining appropriate

constants. The more suitable model to be developed for FRP composite laminate at various temperatures is as follows.

In viscoelastic polymers, the shift factor  $a(T)$  is used to predict the behavior of the tensile viscosity  $\eta(T)$  as well as other mechanical properties such as  $\sigma_{ult}(T)$  and  $E(T)$  of a polymer at various levels of temperatures as:

$$\eta(T) = a(T)\eta(T_0) \quad (3)$$

$$\sigma_{ult}(T) = a_\sigma(T)\sigma_{ult}(T_0) \quad (4)$$

$$E(T) = a_E(T)E(T_0) \quad (5)$$

Material properties at any arbitrary temperature is identified using Eqs. (3-5).  $\sigma_{ult}(T)$  and  $E(T)$  are formulated in laminate FRP composites, and  $a(T)$  is proposed as follows:

$$a(T) = 1 - \frac{C}{\ln\left(1 - \frac{T_0}{T_m}\right)} \ln\left(\frac{1 - \frac{T}{T_m}}{1 - \frac{T_0}{T_m}}\right) \quad (6)$$

$C$  is Constant corresponds to the sensitivity of material or mechanical property with respect to variation of temperature as shown in Eqs. (7-8):

$$C_\sigma = \frac{\sigma_{ult}(0)}{\sigma_{ult}(T_0)} - 1 \quad (7)$$

$$C_E = \frac{E(0)}{E(T_0)} - 1 \quad (8)$$

By substituting Eqs. (7-8) for Eq. (6), Eqs. (4-5) can be rewritten as follows:

$$\sigma_{ult}(T) = \sigma_{ult}(T_0) \left[ 1 - \frac{\frac{\sigma_{ult}(0)}{\sigma_{ult}(T_0)} - 1}{\ln\left(1 - \frac{T_0}{T_m}\right)} \ln\left(\frac{1 - \frac{T}{T_m}}{1 - \frac{T_0}{T_m}}\right) \right] \quad (9)$$

$$E_c(T) = E_c(T_0) \left[ 1 - \frac{\frac{E_c(0)}{E_c(T_0)} - 1}{\ln\left(1 - \frac{T_0}{T_m}\right)} \ln\left(\frac{1 - \frac{T}{T_m}}{1 - \frac{T_0}{T_m}}\right) \right] \quad (10)$$

Eqs. (9-10) are the mathematical models to predict the values of ultimate tensile strength and the Young's modulus of laminated FRP composites at different temperatures. In Eqs. (7-8), where  $\sigma_{ult}(0) \geq \sigma_{ult}(RT)$  and  $E_c(0) \geq E_c(RT)$ , the constant  $C_\sigma$  and  $C_E$  vary between 0 and 1 for most FRP laminate composites. To consider the temperature effect in fatigue damage as shown in Eq. (2), the temperature dependent parameters of  $E_c(T)$  and  $\sigma_{ult}(T)$  have been formulated as shown in Eqs. (9-10). Fatigue life denoted as  $N_f$  at temperature  $T$  was employed as an input of the damage equation. Therefore, considering all the aforementioned parameters, fatigue damage in Eq. (2) is given as:

$$D = \left\{ \left( 1 - \frac{F}{E_c(T)} \right) (1 - f^*) \frac{\ln(N + 1)}{\ln(nN_f)} \right\} + \left\{ \left( 1 - \frac{F}{E_c(T)} \right) f^* \left( \frac{N}{nN_f} \right) \right\} \\ + \left\{ \frac{F}{E_c(T)} \left( 1 - \frac{\sigma_{max}(1-R)}{2\sigma_{ult}(T)} \right) \frac{\ln\left(1 - \frac{N}{nN_f}\right)}{\ln\left(\frac{1}{nN_f}\right)} \right\} \quad (11)$$

where  $F$  changes depend on the lay-up distribution of composite laminates,  $F = V_f^* \cos(\theta)$ ,  $V_f^* = K_f V_f$  corresponds to the volume fraction of fibers aligned in the loading direction.

The damage model reveals the fact that by subtracting the summation of stiffness-reduction values of matrix and fiber from the initial composite stiffness, the stiffness of the composite prior to failure can be obtained. It is under the assumption that the matrix is subjected to severe damage prior to final failure and fibers are degraded up to a critical point where the composite structure loses its integrity.

### 5 Stiffness degradation model for FRP composite laminates with different off-axis angle plies

Eq. (12) presents a general equation that describes the accumulative damage of a typical composite laminate with different off-axis angle plies.

$$\mathbf{D}_{(0/\theta/0)} = \sum \eta_i \mathbf{D}_i \quad (12)$$

Weighting factors  $\eta_i (i = 1, 2, \dots, n)$  are employed to differentiate the efficiency of  $(0/\theta/0)$  load carrying plies of  $\theta$  in the composite laminates. Factor  $\eta$  is quantitatively estimated from experimentally obtained damage value of  $(0/\theta/0)$  plies over the life cycles. At a given number of cycle  $N_i$ , factor  $\eta_i$  is defined as:

$$\eta_\theta = \frac{D_{(0/\theta/0)} - D_{(0)}}{D_{(\theta)} - D_{(0)}} \quad (13)$$

$$\eta_0 = \frac{1}{2} (1 - \eta_\theta) \quad (14)$$

### 6 The analysis model of fatigue damage for FRP composite laminates

Eq. (11) contains terms of matrix damage, fiber-matrix interface and fiber. Based on Eq. (11), the damage analysis procedure includes,

- 1) Define important initial parameters that reveal the mechanical, structural and temperature effect:  $N_f(T), E_m, V_m, F(E_f, V_f, \theta), E_c(T) (E_c(0), E_c(T_0)), T_0, T_m, f^*, \sigma_{appl}, \sigma_{ult}(T) (\sigma_{ult}(0), \sigma_{ult}(T_0)), R(\sigma_{min}, \sigma_{max}), n$
- 2) Calculate the values of damage in individual  $0^\circ$  and  $\theta^\circ$  respectively using Eq. (11),
- 3) Estimate the weighting factor  $\eta_i$  factor and calculate the fatigue damage of  $(0/\theta/0)$  composites using Eqs. (13-14),
- 4) Calculate the accumulative damage of  $(0/\theta/0)$  composite laminates over the whole fatigue life using Eq. (12).

#### 6.1 Property parameters of FRP composites

Tab. 3 shows the basic property of different types of FRP composites.

**Table 3:** Property Parameters of Different Types of FRP Composites

Index	Parameter		CFRP	GFRP	AFRP	BFRP
Fatigue Life	$N_f(T)$	-	$6.34 \cdot 10^4$	$6.15 \cdot 10^4$	$5.97 \cdot 10^4$	$6.12 \cdot 10^4$
Young's Modulus of Matrix	$E_m(GPa)$	-	3.3	4.73	3.58	4.06
Volume Fraction of Matrix	$V_m$	-	0.35	0.38	0.30	0.43
Term		$F$	-	-	-	-
Young's Modulus of Fiber	$E_f(GPa)$	-	228	82	113	97
Volume Fraction of Fiber	$V_f$	-	0.55	0.49	0.58	0.53
Off-axis Angle	$\theta$	-	-	-	-	-
Young's Modulus of Composite	-	$E_c(T)$	-	-	-	-
Young's Modulus of Composite (0)	$E_c(0)(GPa)$	-	198	48	145	92
Young's Modulus of Composite ( $T_0$ )	$E_c(T_0)(GPa)$	-	187	43	136	84
Room Temperature	$T_0(K)$	-	295	296	295	294
Polymer Melting Point	$T_m(K)$	-	448	450	453	446
Fiber-Matrix Interface Strength	$f^*$	-	0.51	0.50	0.48	0.52
Applied Tensile Fatigue Stress	$\sigma_{appl}(MPa)$	-	153	119	104	137
Ultimate Tensile Stress	-	$\sigma_{ult}(T)$	-	-	-	-
Ultimate Tensile Stress(0)	$\sigma_{ult}(0)(MPa)$	-	2012	1320	1148	1608
Ultimate Tensile Stress ( $T_0$ )	$\sigma_{ult}(T_0)(MPa)$	-	1854	1100	903	1409
Stress Ratio	-	$R$	0.098	0.099	0.097	0.10
Minimum Fatigue Stress	$\sigma_{min}(MPa)$	-	16.2	12.9	11.6	14.2
Maximum Fatigue Stress	$\sigma_{max}(MPa)$	-	166	130	120	139
Percentage of Drop in Stiffness	$n$	-	1.66	1.67	1.69	1.66

Remark: The actual values of the parameters of different types of FRP composites are different according to various manufacturers. The parameters in the Tab. 3 are chosen or extrapolated from general or typical FRP composite material [Wharmby, Ellyin and Wolodko (2003); Lian and Yao (2010); Philippidis and Vassilopoulos (1999); Varvani-Farahani, Haftchenari and Panbechi (2007); Shirazi and Varvani-Farahani (2010)].

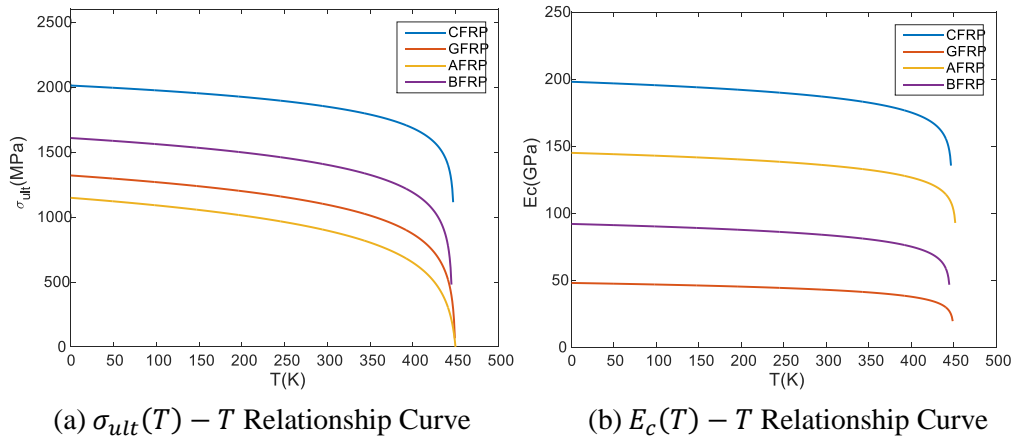
**6.2 Parameter study of comparative FRP unidirectional composites**

From Eqs. (9-11), we know that  $\sigma_{ult} - T, E_c - T$  relationship curves of four types of FRP composites (CFRP, GFRP, AFRP, BFRP). From the Fig. 2, we know that  $\sigma_{ult}(T)$  and  $E_c(T)$  are closely related with temperature  $T$ , and these parameters are mainly dominated by matrix. Especially when the temperature is near the melting point of matrix, the curves drop abruptly.

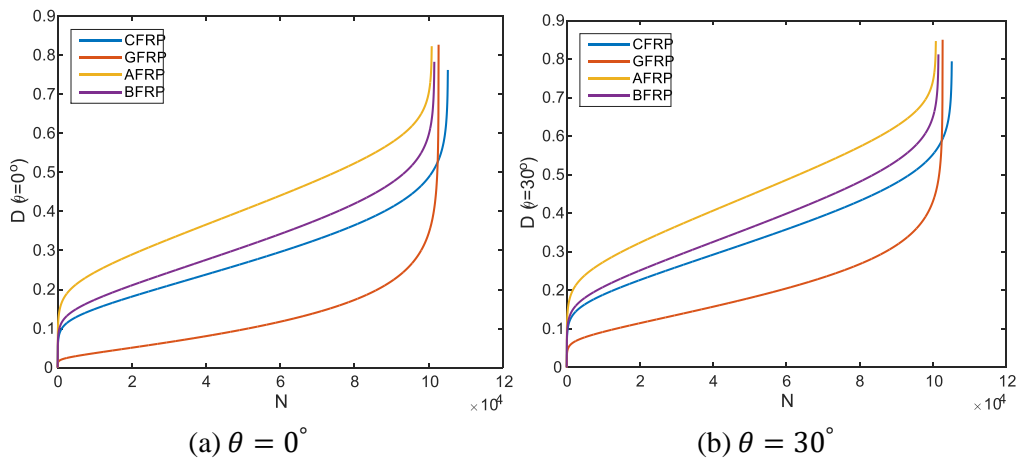
When  $T = T_0, D - N$  accumulative fatigue damage (Fig. 3) is closely related with the term  $F$  with respect to the fiber mechanical properties and the fatigue life  $N = nN_f$ , and

the curve rises abruptly when the off-axis approximates  $90^\circ$ , in which case the matrix bonding strength is the dominant factor that determines the quantity of damage.  $K_f$  regarding the term  $F$  in the accumulative fatigue damage equation is proposed for this specific case, and for orthogonal woven composites, the term  $F$  can be modified as  $K_f E_f V_f$ .

Level three headings should be in italic, and be flushed to the left. Similarly, the level three headings should be numbered after the level two headings, such as 3.2.1, 3.2.2, etc.



**Figure 2:** A Comparison of Thermal Relationship Curve between different types of FRP composite



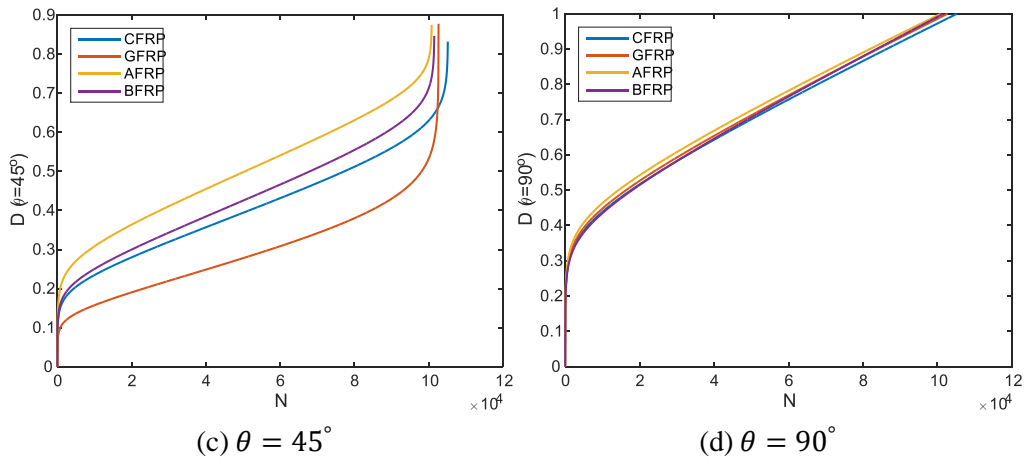


Figure 3: D-N Fatigue Damage,  $T = T_0$ .

When  $T=T_0$ ,  $D-\theta-N$  reflects the accumulative fatigue damage versus off-axis angle  $\theta$  and fatigue cycle  $N$ , as shown in Fig. 4.

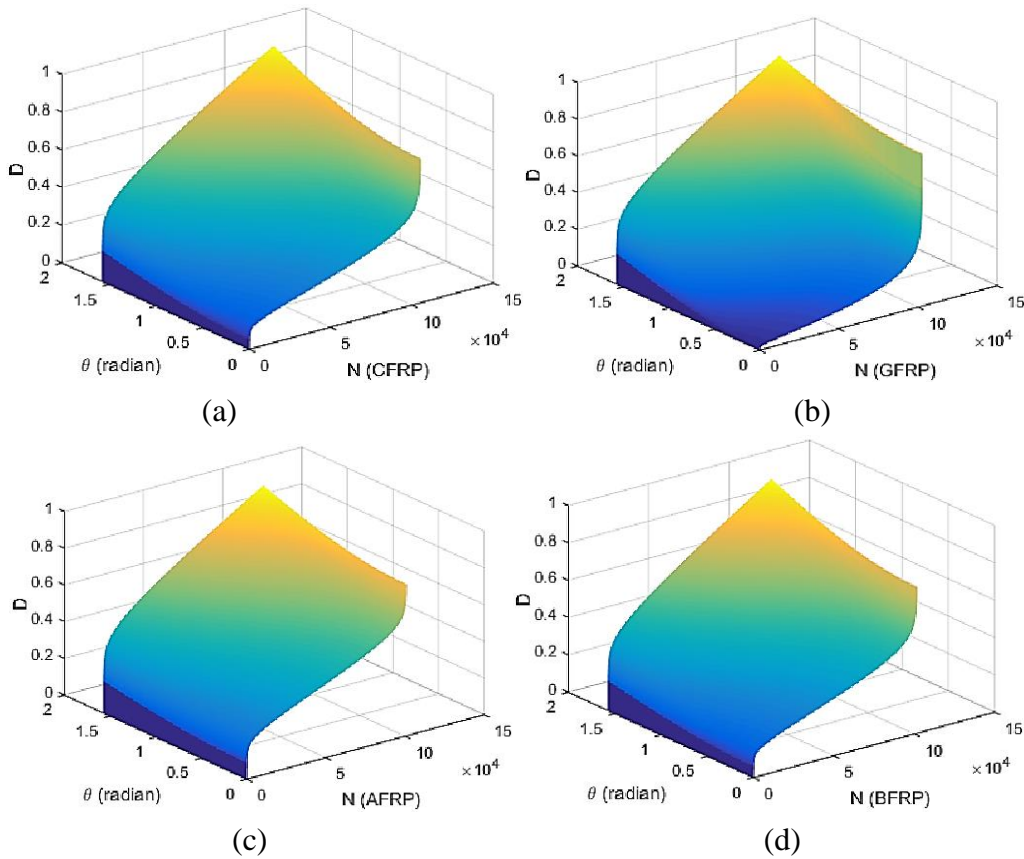
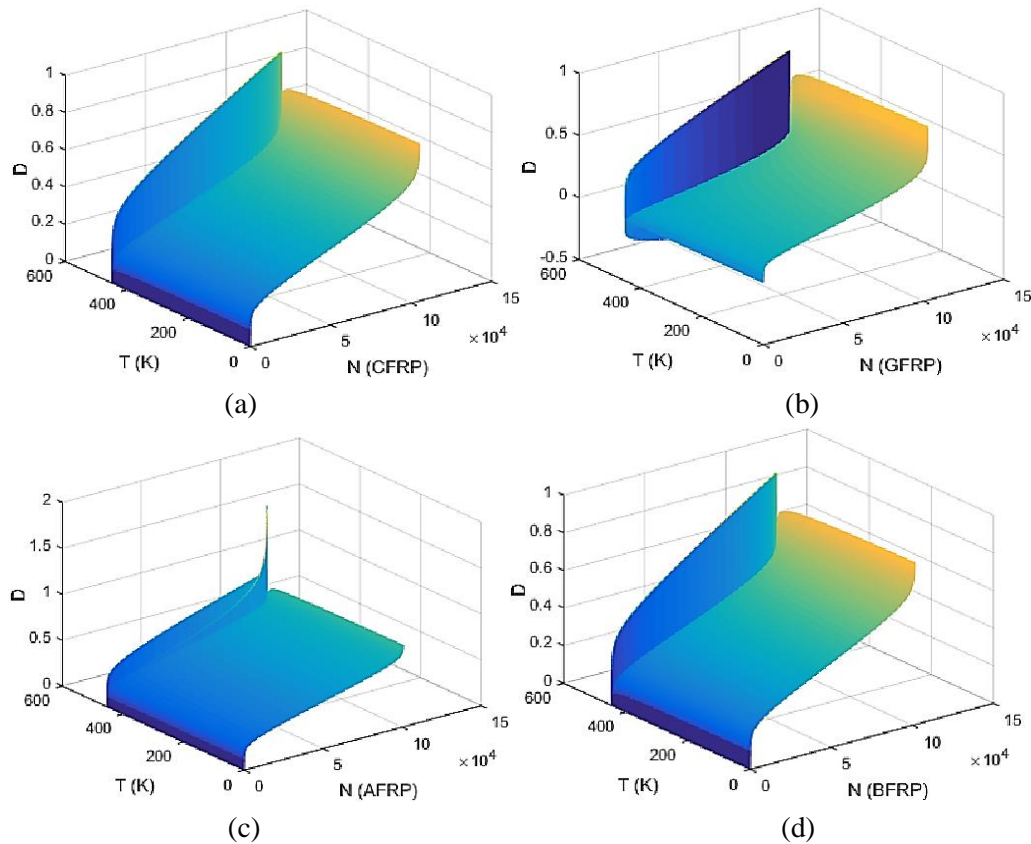


Figure 4:  $D - \theta - N$  Fatigue Damage (a) CFRP (b) GFRP (c) AFRP (d) BFRP

When the off-axis angle  $\theta = 45^\circ$ ,  $D - T - N$  reflects the accumulative fatigue damage versus temperature  $T$  and fatigue cycle  $N$ , as shown in Fig. 5. When approaching the melting point of the matrix, the accumulative fatigue damage increases significantly.



**Figure 5:** D-T-N Fatigue Damage (a) CFRP (b) GFRP (c) AFRP (d) BFRP

**6.3 Comparative parameter study of FRP composite laminates using control variate method**

According to the experimental work and empirical deduction, Fig. 6 shows that the variation of this factor is steady with a small decay over life cycles. Tab. 4 lists factor  $\eta$  versus fatigue cycles for different types of FRPs.

**Table 4:**  $\eta$  Values for Different Types of FRP Laminates

$\eta$	CFRP	GFRP	AFRP	BFRP
$(0^\circ/30^\circ/0^\circ)$	0.32	0.34	0.33	0.32
$(0^\circ/45^\circ/0^\circ)$	0.52	0.54	0.49	0.50
$(0^\circ/90^\circ/0^\circ)$	0.20	0.22	0.20	0.21

Indicated by Eqs. (9-14), when  $T = T_0$ ,  $D - N$  accumulative fatigue damage versus fatigue life for the specific off-axis angle but different FRP composite laminates can be shown in Fig. 7.

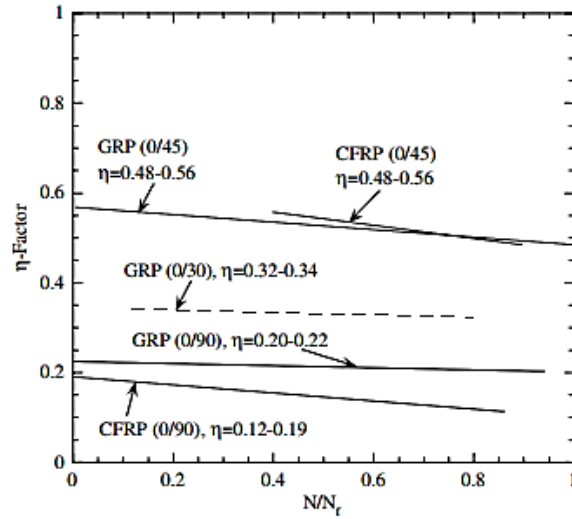
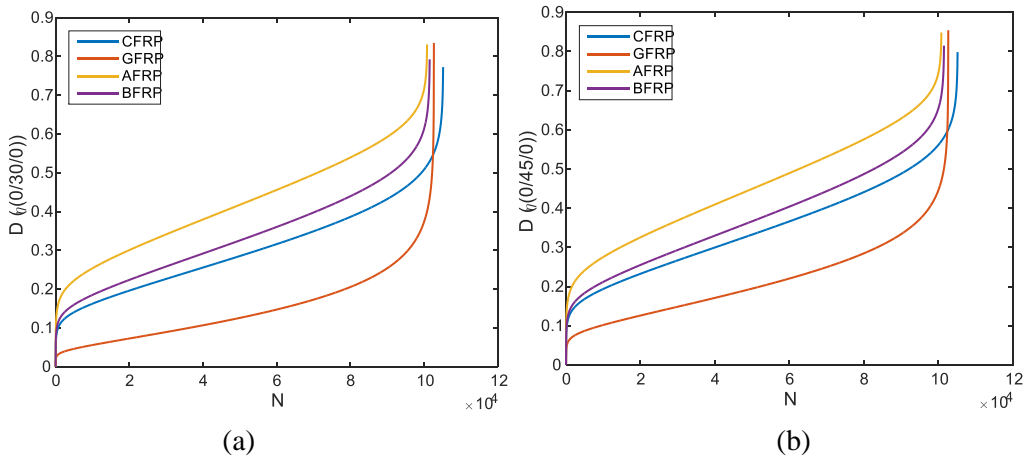
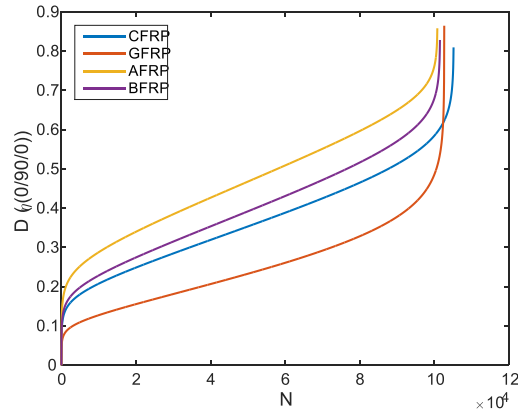


**Figure 6:** Factor  $\eta$  versus Fatigue Cycles



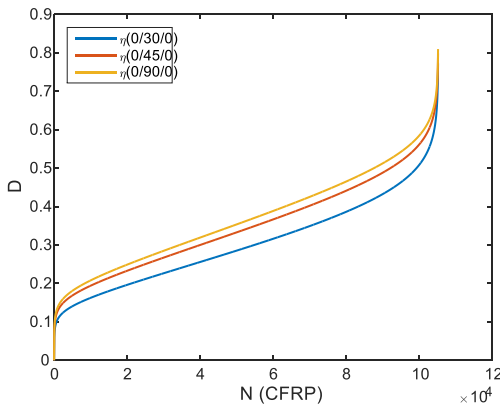
(a)

(b)

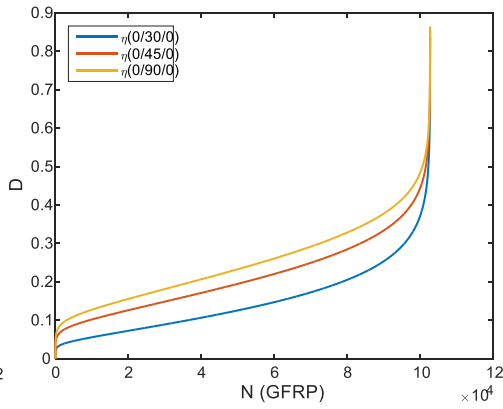


(c)

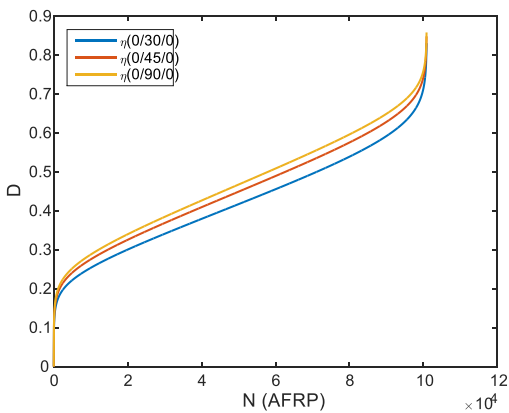
**Figure 7:**  $D - N$  Fatigue Damage (a) (0/30/0) (b) (0/45/0) (c) (0/90/0).



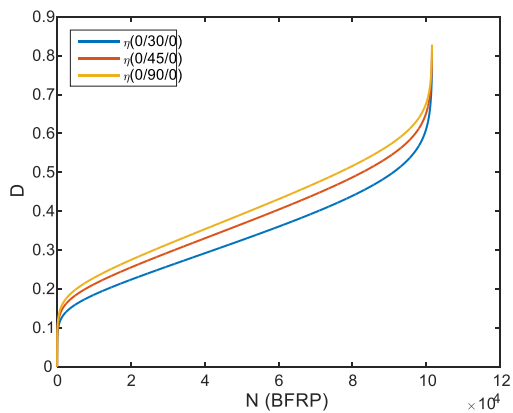
(a)



(b)



(c)



(d)

**Figure 8:**  $D - N$  Fatigue Damage (a) CFRP (b) GFRP (c) AFRP (d) BFRP

When  $T = T_0$ ,  $D - N$  accumulative fatigue damage versus fatigue life for the specific FRP type but different off-axis angles.

We know from Fig. 8 that though the weighting factor  $\eta_{(0/45/0)} > \eta_{(0/30/0)} > \eta_{(0/90/0)}$  according to the experimental work and empirical deduction, the fatigue accumulative damage  $D\eta_{(0/90/0)} > D\eta_{(0/45/0)} > D\eta_{(0/30/0)}$ , which means the larger the off-angle axis is, the larger possibility the damage occurs for the same case, and this also demonstrates the main strength is determined by off-axis direction of fibers within composite laminates.

#### **6.4 Discussions of the proposed fatigue damage model for composite laminates**

As clearly discussed above, For a specific composite laminate with (0/θ/0) ply direction under cyclic loading, the relationship between the drop in stiffness and the number of cycles also shows three different regions, following the mechanism of damage of FRP composites, i.e. at the first stage, matrix cracks occurs, and second stage, the interface between matrix and fiber encounters, and in the third stage, fiber breakage result in catastrophic failure. Matrix is the dominant factor determined by temperature, while fiber strength is the dominant factor that determine the reliability of composite.

#### **7 Conclusions and recommendations for further research**

This paper extends previous work of the study on accumulative fatigue damage model based on material stiffness reduction for composite laminates. Fatigue evolution mechanism and theoretical models for different types of FRP composite (CFRP, GFRP, AFRP and AFRP) laminates are presented and discussed. Experimental work will be further conducted to verify the reliability and applicability of the fatigue damage model. According to the fatigue damage model, a FRP composite pipeline system will be built in a coupled field environment in the future work, and electrical capacitance sensors will be used as exciting and measuring electrodes to detect the electrostatic variation, and some frequency based damage indicators will be proposed.

**Acknowledgement:** This work is now supported by a Structural Health Monitoring R&D Project (No. 2017YFC0805103), and Post-doc funds (No. 1105000384, No. 2018K133C), a Thousand Talent Program, Jiangsu Shuangchuang Program, and was supported by 973 Project “Fundamental Research on Applied FRP to Realize High Performance and Longevity in Major Infrastructure Systems” (No. 2012CB026200).

#### **Notation:**

$D$	Cumulative fatigue damage of composites,
$E_N$	Young’s modulus of the damaged composite in $N^{\text{th}}$ cycle,
$E_0$	Initial Young’s modulus for undamaged composite,
$E_m$	Young’s modulus of matrix component,
$E_f$	Young’s modulus of fiber component,

$E_c$	Young's modulus of composite contracture,
$V$	Volume fraction,
$V_f$	Volume fraction of fiber component,
$V_m$	Volume fraction of matrix component,
$\sigma_{ult}$	Ultimate value of tensile stress,
$\sigma_{appl}$	Applied tensile that indicates the strengthness of fatigue stress,
$\sigma_{max}$	Maximum value of applied stress,
$\sigma_{min}$	Minimum value of applied stress,
$R(\sigma_{min}/\sigma_{max})$	Stress ratio,
$\sigma_a$	Amplitude stress,
$N$	Number of loading cycles,
$N_f$	Number of cycles due to fatigue loading,
$\theta$	Fiber orientation,
$T$	Temperature effect,
$T_0$	Reference temperature,
$T_g$	Supposed temperature,
$T_m$	Melting temperature of composite polymer,
$E(T)$	Young's modulus with temperature varying,
$E(T_0)$	Young's modulus at the specific reference temperature,
$E(0)$	Young's modulus at absolute zero temperature,
$\sigma_{ult}(T)$	Ultimate tensile strength at specific reference,
$\sigma_{ult}(T_0)$	Ultimate tensile strength with temperature varying,
$\sigma_{ult}(0)$	Ultimate tensile strength at absolute zero temperature,
$\eta(T_0)$	Tensile viscosity at specific reference,
$a_\sigma(T)$ and $a_E(T)$	Corresponding material shift factors with temperature varying,
$K, c$	Material constants,
$a(T)$	Corresponds to the shift factor obtained from the WLF and Arrhenius equations,
$f^*$	parameter indicating the strength of the interface between fiber and matrix ( $0 \leq f^* \leq 1$ ), for $f^* = 0$ , fiber-matrix interface strength (FMIS) is very low, and for $f^* = 1.0$ , FMIS improves in strength,
$n$	Percentage of stiffness reduction assumed for a specific fatigue test, e.g. if the degradation up to 60% damage of real fatigue life, $n = (0.6)^{-1} = 1.67$ , $nN_f = 1.67N_f$

## References

- Abouelwafa, M. N.; El-Gamal, H. A.; Mohamed, Y. S.; Altabey, W. A.** (2014): An expert system for life prediction of woven-roving GFRE closed end thick tube subjected to combined bending moments and internal hydrostatic pressure using artificial neural network. *Advanced Materials Research*, vol. 845, pp. 12-17.
- Adediran, O. A.; Abdel Wahab, M. M.; Xu, W.; Crocombe, A. D.** (2018): Application of FE model updating for damage assessment of FRP composite beam structure. *Topics in Modal Analysis II*, vol. 6, pp. 385-398.
- Altabey, W. A.** (2014): Vibration analysis of laminated composite variable thickness plate using finite strip transition matrix technique and MATLAB verifications. *MATLAB Applications for the Practical Engineer*.
- Altabey, W. A.** (2017): An exact solution for mechanical behavior of BFRP Nano-thin films embedded in NEMS. *Advances in Nano Research*, vol. 5, no. 4, pp. 337-357.
- Altabey, W. A.** (2017a): Delamination evaluation on basalt FRP composite pipe by electrical potential change. *Advances in Aircraft and Spacecraft Science*, vol. 4, no. 5, pp. 515-528.
- Altabey, W. A.** (2017a): Free vibration of basalt fiber reinforced polymer (FRP) laminated variable thickness plates with intermediate elastic support using finite strip transition matrix (FSTM) method. *Vibroengineering*, vol. 19, no. 4, pp. 2873-2885.
- Altabey, W. A.** (2017b): EPC method for delamination assessment of basalt FRP pipe: electrodes number effect. *Structural Monitoring and Maintenance*, vol. 4, no. 1, pp. 69-84.
- Altabey, W. A.** (2017b): Prediction of natural frequency of basalt fiber reinforced polymer (FRP) laminated variable thickness plates with intermediate elastic support using artificial neural networks (ANNs) method. *Vibroengineering*, vol. 19, no. 5, pp. 3668-3678.
- Altabey, W. A.** (2018): High performance estimations of natural frequency of basalt FRP laminated plates with intermediate elastic support using response surfaces method. *Vibroengineering*, vol. 20, no. 2, pp. 1099-1107.
- Altabey, W. A.; Noori, M.** (2017): Detection of fatigue crack in basalt FRP laminate composite pipe using electrical potential change method. *Journal of Physics: Conference Series*, vol. 842, 012079.
- Altabey, W. A.; Noori, M.** (2017): Fatigue life prediction for carbon fibre/epoxy laminate composites under spectrum loading using two different neural network architectures. *Sustainable Materials and Structural Systems*, vol. 3, no. 1, pp. 53-78.
- Altabey, W. A.; Noori, M.** (2018): Monitoring the water absorption in GFRE pipes via an electrical capacitance sensors. *Advances in Aircraft and Spacecraft Science*, vol. 5, no. 4, pp. 411-434.
- Carraro, P. A.; Quaresimin, M.** (2014): A damage based model for crack initiation in unidirectional composites under multiaxial cyclic loading. *Composites Science and Technology*, vol. 99, pp. 154-163.
- Chen, Z. F.; Wan, L. L.; Lee, S.; Ng, M.; Tang, J. M. et al.** (2008): Evaluation of CFRP, GFRP and BFRP Material Systems for the Strengthening of RC Slabs. *Reinforced Plastics and Composites*, vol. 27, no. 12, pp. 1233-1243.

- Coronado, C. A.; Lopez, M. M.** (2010): Numerical modeling of concrete-FRP debonding using a crack band approach. *Composites for Construction*, vol. 14, no. 1, pp. 11-21
- Das, R.; Pradhan, R. B.** (2013): Delamination damage analysis of laminated bonded tubular single lap joint made of fiber-reinforced polymer composite. *Damage Mechanics*, vol. 23, no. 6, pp.772-790.
- DasN, R. R.; Baishya, N.** (2016): Failure analysis of bonded composite pipe joints subjected to internal pressure and axial loading. *Procedia Engineering*, vol. 144, pp.1047-1054.
- Eliopoulos, E. N.; Philippidis, T. P.** (2011a): A progressive damage simulation algorithm for GFRP composites under cyclic loading. Part 1 material constitutive model. *Composites Science and Technology*, vol. 71, no. 5, pp. 742-749.
- Eliopoulos, E. N.; Philippidis, T. P.** (2011b): A progressive damage simulation algorithm for GFRP composites under cyclic loading. Part 2 FE implementation and model validation. *Composites Science and Technology*, vol. 71, no. 5, pp. 750-757.
- Guedes, R. M.** (2008): Creep and fatigue lifetime prediction of polymer matrix composites based on simple cumulative damage laws. *Composites Part A, Applied Science and Manufacturing*, vol. 39, no. 11, pp.1716-1725.
- Kennedy, C. R.; O'Bradaigh, C.; Leen, S. B.** (2013): A multi-axial fatigue damage model for fibre reinforced polymer composites. *Composite Structures*, vol. 106, pp. 201-210.
- Lian, W.; Yao W.** (2010): Fatigue life prediction of composite laminates by FEA simulation method. *Fatigue*, vol. 32, no. 1, pp. 123-133.
- Liu, Y.; Shao, X.; Han, X.; Zhuang C.** (2009): Failure types of FRP pipe in oil and gas engineering. *International Conference on Pipelines and Trenchless Technology*.
- Mazzucco, G.; Salomoni, V. A.; Majorana, C. E.** (2012): Three-dimensional contact-damage coupled modelling of FRP reinforcements-Simulation of delamination and long-term processes. *Computers & Structures*, vol. 110-111, pp. 15-31.
- Mivehchi, H.; Varvani-Farahani, A.** (2010): The effect of temperature on fatigue damage of FRP composites. *Materials Science*, vol. 45, no. 14, pp. 3757-3767.
- Philippidis, T. P.; Vassilopoulos, A. P.** (1999): Fatigue of composite laminates under off-axis loading. *Fatigue*, vol. 21, no. 3, pp. 253-262.
- Plumtree, A.; Shi, L.** (2002): Fatigue damage evolution in off-axis unidirectional CFRP. *International Journal of Fatigue*, vol. 24, no. 2-4, pp. 155-159.
- Praveen, G. N.; Reddy, J. N.** (1995): Stiffness reduction mechanisms in composite laminates, IUTAM Symposium on Microstructure-Property. *Interactions in Composite Materials*, pp. 301-312
- Ruocci, G.; Argoul, P.; Benzarti, K.; Freddi, F.** (2013): An improved damage modelling to deal with the variability of fracture mechanisms in FRP reinforced concrete structures. *Adhesion and Adhesives*, vol. 45, pp. 7-20.

**Shirazi, A.; Varvani-Farahani, A.** (2010): A stiffness degradation based fatigue damage model for FRP composites of  $(0, \theta)$  laminate systems. *Applied Composite Materials*, vol. 17, no. 2, pp. 137-150.

**Shiri, S.; Yazdani, M.; Pourgol-Mohammad, M.** (2015): A fatigue damage accumulation model based on stiffness degradation of composite materials. *Materials & Design*, vol. 88, no. 25, pp. 1290-1295.

**Sun, C. Q.; Zhang, J. Y.; Fei, B. J.** (2011): Progressive Damage Model of FRP Composite Laminates with Central Hole. *Advanced Materials Research*, vol. 194-196, pp. 1581-1585.

**Varvani-Farahani, A.; Haftchenari, H.; Panbechi, M.** (2006): A fatigue damage parameter for life assessment of off-axis unidirectional GRP composites. *Composite Materials*, vol. 40, no. 18, pp. 1659-1670.

**Varvani-Farahani, A.; Haftchenari, H.; Panbechi, M.** (2007): An energy-based fatigue damage parameter for off-axis unidirectional FRP composites. *Composite Structures*, vol. 79, no. 3, pp. 381-389.

**Varvani-Farahani, A.; Shirazi, A.** (2007): A fatigue damage model for  $(0, 90)$  FRP composites based on stiffness degradation of  $0^\circ$  and  $90^\circ$  composite plies. *Reinforced Plastics and Composites*, vol. 26, no. 13, pp. 1319-1336.

**Wharmby, A. W.; Ellyin, F.; Wolodko, J. D.** (2003): Observations on damage development in fiber reinforced polymer laminates under cyclic loading. *International Journal of Fatigue*, vol. 25, no. 5, pp. 437-446

**Zeng, Q.; Wang, Z.; Ling L.** (1997): A study of the influence of interfacial damage on stress concentrations in unidirectional composites. *Composites Science and Technology*, vol. 57, no. 1, pp. 129-135.

**Zhao, Y.; Noori, M.; Altabey, W. A.; Zhishen, W.** (2018): Fatigue damage identification for composite pipeline systems using electrical capacitance sensors. *Smart Materials and Structures*, vol. 27, no. 8.